Vortex state in ferromagnetic nanoparticles

Davide Betto and J. M. D. Coey

Citation: Journal of Applied Physics **115**, 17D138 (2014); doi: 10.1063/1.4867597
View online: http://dx.doi.org/10.1063/1.4867597
View Table of Contents: http://scitation.aip.org/content/aip/journal/jap/115/17?ver=pdfcov
Published by the AIP Publishing

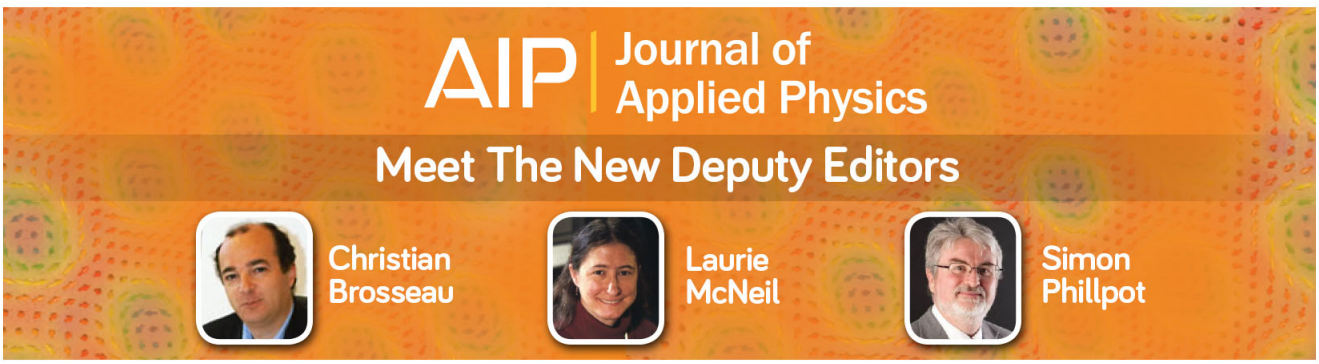

Vortex state in ferromagnetic nanoparticles

Davide Betto[a] and J. M. D. Coey
CRANN and School of Physics, Trinity College, Dublin 2, Ireland

(Presented 5 November 2013; received 20 September 2013; accepted 29 November 2013; published online 5 March 2014)

The evolution of the magnetic state of a soft ferromagnetic nanoparticle with its size is usually thought to be from superparamagnetic single domain to blocked single domain to a blocked multidomain structure. Néel pointed out that a vortex configuration produces practically no stray field at the cost of an increase in the exchange energy, of the order of $RJS^2 \ln R/c$, where JS^2 is the bond energy, R is the particle radius, and c is of the order of the exchange length. A vortex structure is energetically cheaper than single domain when the radius is greater than a certain value. The correct sequence should include a vortex configuration between the single domain and the multidomain states. The critical size is calculated for spherical particles of four important materials (nickel, magnetite, permalloy, and iron) both numerically and analytically. A vortex state is favored in materials with high magnetisation.
 [http://dx.doi.org/10.1063/1.4867597]

I. INTRODUCTION

Magnetic nanoparticles (NPs) are important in many fields, ranging from paleomagnetism to biomedical imaging to sensors. They can be fabricated by a variety of chemical methods in various sizes and shapes.[5,9] It is not easy to isolate and analyse a single NP, since they usually come in assemblies of several thousands. In this case, the interactions between different NPs are not negligible and interparticle dipolar intercation may determine the magnetic state of the whole cluster. In this paper, we focus on the magnetic configurations of a single, isolated NP of a soft ferromagnetic material, with a radius above the superparamagnetic limit. The characteristics of the vortex state (Fig. 1) have been extensively investigated for cylindrical nanodots,[4,10,11] while it has not yet been observed in arrays of spherical NPs.[1,6]

II. THEORY

A. Vortex state

We first consider a 2D circular plane with a vortex configuration. In the micromagnetic approach, we express the (normalised) spin vectors $\vec{m}$ in spherical coordinates with respect to the $\vec{z}$ axis. Hence, $\vec{m} = \{\sin\theta\cos\phi; \sin\theta\sin\phi; \cos\theta\}$, where θ and ϕ are the polar and azimuthal angles, respectively. Since the structure has cylindrical symmetry, we use cylindrical coordinates in the x-y plane, where the vortices lie, $\vec{x} = \{\rho\cos\varphi; \rho\sin\varphi\}$, with radius ρ and azimuthal angle φ.

From the minimisation of the exchange energy with a variational calculation,[11] it is possible to obtain the relationship between the angle θ and the radius ρ

$$\theta(\rho) = 2\tan^{-1}(\rho/c)\,, \tag{1}$$

where c is the radius of the vortex core. When $\rho = c$, we have $\theta = \pi/2$; hence, the magnetisation is completely in plane.

The exchange energy of the 2D vortex of radius R is given by the integral

$$E_{exch} = \int_0^{2\pi} d\varphi \int_0^R \rho\, d\rho \frac{A}{2}\left[\left(\frac{\partial\theta}{\partial\rho}\right)^2 + \frac{\sin^2\theta}{\rho^2}\right], \tag{2}$$

where A is the exchange constant. The total exchange energy is given by the sum of two terms, one representing the core and the other representing the outer ring. Integrating Eq. (2) from $z = -R$ to $z = R$, we obtain the energy for a 3D sphere as

$$E_{exch} = 2\pi RA\left(1 + \ln\frac{R}{c}\right). \tag{3}$$

Next, we consider the energy arising from uniaxial anisotropy with anisotropy constant K_1. The first case, we discuss is when the easy axis is in the $\vec{z}$ direction. Then

$$E^z_{ani} = \frac{2\pi K_1 R^3}{3} + 4\pi R K_1 c^2\left(2\ln 2 - \frac{3}{2}\right). \tag{4}$$

When the easy axis is in-plane (without loss of generality, we consider it to be the $\vec{y}$ axis), the angle between the magnetisation and the axis is φ. Then, the energy is given by

$$E^x_{ani} = \frac{K_1\pi}{3}R^3 - K_1\pi R c^2(\ln 16 - 2)\,. \tag{5}$$

The self-energy arising from the demagnetising field can be calculated using the magnetic charge approach. The only charges come from the core spins on the upper and lower polar circles. The magnetic charge density is given by the formula $\sigma = \vec{m}\cdot\vec{n}$, where $\vec{n}$ is a vector normal to the surface. The main contribution comes from charges on the same circle (upper or lower). Using spherical coordinates for the position on the surface of the sphere $\vec{m} = \{\sin\vartheta\cos\varphi; \sin\vartheta\sin\varphi; \cos\vartheta\}$, we have then $\sigma(\vartheta) = \cos(\theta - \vartheta)$. The distance between two points on the surface can be given as a function of the difference of the two azimuthal angles $\Delta\vartheta = \vartheta_1 - \vartheta_2$. The result is

[a]Electronic mail: bettod@tcd.ie.

$$E_{demag} = \frac{\mu_0 M_S^2}{\sqrt{2}R}\int_0^{2\pi} d\varphi_1 \int_0^{2\pi} d\varphi_2 \int_{a/r}^{\vartheta_{max}-a/R} \sin\vartheta d\vartheta \int_{-\vartheta}^{\vartheta_{max}-\vartheta} \sin(\vartheta+\Delta\vartheta) d\Delta\vartheta \times \frac{\cos\left(2\tan^{-1}\left(\frac{R\sin\vartheta}{c}\right)-\vartheta\right)\cos\left(2\tan^{-1}\left(\frac{R\sin(\vartheta+\Delta\vartheta)}{c}\right)-(\vartheta+\Delta\vartheta)\right)}{\sqrt{1-\cos\vartheta\cos(\vartheta+\Delta\vartheta)-\cos(\varphi_1-\varphi_2)\sin\vartheta\sin(\vartheta+\Delta\vartheta)}}, \quad (6)$$

where $\vartheta_{max} = \sin^{-1}(c/R)$ and c is a constant of the order of the exchange length $\sqrt{A/\mu_0 M_S^2}$. In order to avoid divergence when $\Delta\vartheta \to 0$, the integral (6) must be split into two parts. The first part is the integral of $\Delta\vartheta$ between a/R and $\vartheta_{max} - \vartheta$ (positive values), while the second part covers $-\vartheta < \Delta\vartheta < -a/R$ (negative values). The total demagnetising energy has been numerically estimated for a number of core radii as shown in Fig. 2.

B. Uniform magnetisation

Since all the spins are parallel to each other the exchange energy is zero. The only important term arises from the demagnetising energy. The demagnetising factor for a sphere is $N = -1/3$ in all directions, since they are all equivalent. Hence, the demagnetising energy is

$$E_{demag} = -\frac{\mu_0}{2}\int_V \vec{H}_{demag}\cdot\vec{M}dV = \frac{2}{9}\mu_0\pi M^2 R^3. \quad (7)$$

III. SIMULATION DETAILS

Micromagnetic simulations for ferromagnetic NPs in the macrospin approximation had been performed using the OOMMF package. We have used a cellsize of 2 nm for the generation of the mesh. This scale is smaller than the exchange length for all materials considered, but not so small as to give unrealistic results. We have repeated some simulations with smaller and bigger cell size and, apart from calculation times, we have obtained the same results. The other parameters for the different materials are listed in Table I.

In the the first one, the initial configuration of the magnetisation is uniform along the z axis, which is the uniaxial magneto-crystalline anisotropy axis. In the second one it is a random orientation of the magnetic moment for each cell of the mesh. Hence, the first case represents the relaxation to the ground state after having saturated the NP with a high enough external field. The second condition can be obtained by letting the particle cool down from above its Curie temperature in zero field. The results are listed in Table II.

As expected, a vortex structure is present for the particles with larger radius. The orientation of the vortex core is random for materials with very low anisotropy. In the case of uniaxial anisotropy, the core tends to be perpendicular to the easy axis so that at least some in-plane spins of the vortices (which represent the majority of the total spins) will lie parallel to this axis. In the case of cubic anisotropy, the core is oriented in one of the hard directions. This has been verified for nickel: An initial magnetisation along $\vec{x}$, $\vec{y}$, or $\vec{z}$ has always ended up with a vortex state with the core aligned along the hard $\vec{z}$ axis. In the case of no anisotropy the core axis stays aligned with the initial direction of the magnetisation. The radius of the core is not constant in the volume. It is bigger in the centre and smaller at the top and bottom of the particles. This is

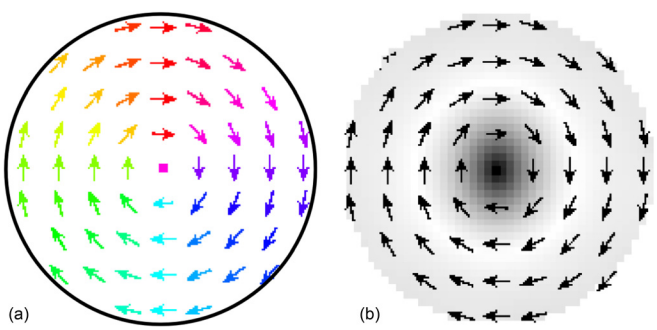

FIG. 1. Vortex state. In (a), the colorcode represents the x-y angle of the magnetisation vectors, while in (b) it represents the z component, showing the core in the centre.

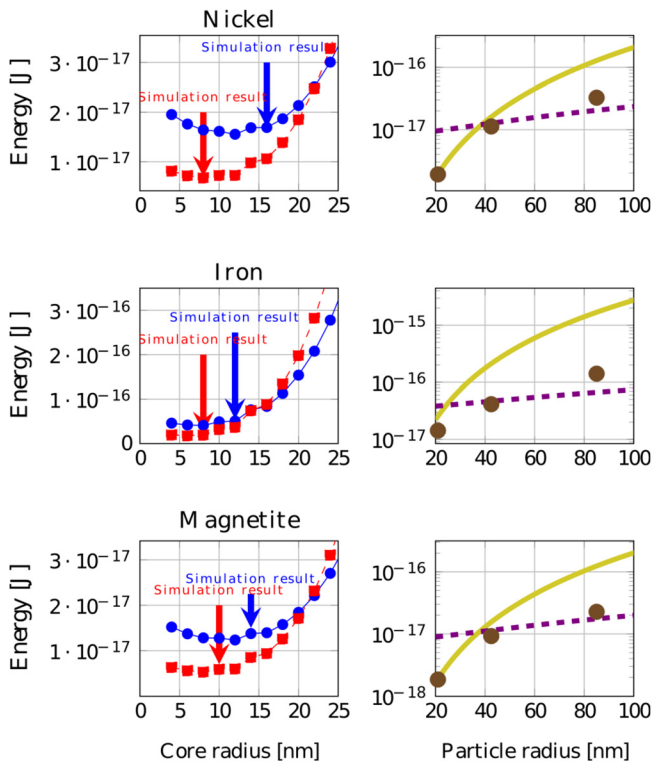

FIG. 2. Comparison between OOMMF simulations and analytical calculations. In the left column, filled blue circles and filled red squares correspond to the analytically calculated energy, discretised as described in Sec. II, for particle radii of 85 and 42.5 nm, respectively. Arrows indicate OOMMF results. The right column shows the total energy for the vortex state (violet dashed) and the uniform magnetisation (yellow solid) as a function of the particle size. The dots indicate the results from OOMMF simulations.

TABLE I. Parameters for micromagnetic simulations.

Material	M_S (kA m^{-1})	A (J m^{-1})	K_{1c} (J m^{-3})
Nickel	488	9×10^{-12}	-5×10^{-3}
Iron	1770	21×10^{-12}	48×10^{-3}
Magnetite	480	7×10^{-12}	-13×10^{-3}
Permalloy	830	10×10^{-12}	-1×10^{-3}

reasonable since the out-of-plane magnetisation of the core produces stray field only at the surface of the particle. Hence, a slightly bigger core in the centre decreases the overall exchange energy.

IV. SIMULATIONS AND ANALYTICAL RESULTS COMPARISON

The core radius can be obtained by minimising the energy of the vortex structure. In the OOMMF simulations, it is bigger in the centre as discussed in Sec. III. We have also simulated the behaviour of a NP in the vortex state with the field applied perpendicular to the core axis. The results show the typical vortex response reported by various authors,[4,6] where at the fields corresponding to the nucleation-annihilation of the vortex the magnetisation loop is not reversible, in agreement with earlier results. A comparison of the calculations and the simulations is shown in Fig. 2.

TABLE II. Results of micromagnetic simulations.

Radius (nm)	Initial conf	Final conf	Energy (10^{-18} J)	Core radius (nm)
		Nickel		
21	Random/uniform	Uniform	1.903	none
42.5	Uniform	Uniform	16.04	none
42.5	Random	Vortex[a]	11.52	~10
85	Uniform	Vortex[b]	32.70	~18
		Iron		
21	Uniform	Uniform	24.95	none
21	Random	Vortex	14.23	~8
42.5	Uniform	Vortex	41.40	~10
42.5	Random	Vortex	41.40	~10
85	Uniform	Vortex	140.6	~14
85	Uniform (hard plane)[c]	Vortex	140.6	~14
85	Random	Vortex[a]	142.3	~14
		Magnetite		
21	Uniform	Uniform	1.841	none
21	Random	Uniform	1.841	none
42.5	Uniform	Uniform	15.52	none
42.5	Random	Vortex	9.224	~12
85	Random/uniform	Vortex	22.69	~16
		Permalloy		
21	Uniform	Uniform	5.497	none
21	Random	"C" curl	4.901	none
42.5	Random/uniform	Vortex	14.21	~12
85	Uniform	Vortex	33.40	~16
85	Random	Vortex	32.39	~16

[a]In this case the vortex core is not always in the centre of the particle but it is displaced and moves from one side to the other in the volume.
[b]The vortex axis aligns with the hard axis regardless of the initial direction of the saturated magnetisation. In the case with no anisotropy, the vortex axis aligns with the initial direction of the magnetisation.
[c]Uniform magnetisation aligned in the hard plane.

V. DISCUSSION AND CONCLUSIONS

Similar numerical simulations have been performed in the past, especially by Fredkin and Koehler.[7] They used a tetrahedral mesh and a random distribution of points for the finite element discretization. Their results are qualitatively in agreement with ours when describing the characteristics of the vortex state and its behaviour while sweeping a external magnetic field. However, their range of material parameters was substantially different from ours. For one set of values which can be compared to our NPs, they found a vortex structure, in agreement with our result. Brown[8] discussed the upper and lower radii resulting in non-uniform or uniform magnetisation, respectively. He found that below 19.77, 8.33, 17.33, and 12.25 nm for Ni, Fe, magnetite, and permalloy, respectively, the magnetisation is uniform, in reasonable agreement with our findings. Above 26.09, 10.84, 25.75, and 15.44 nm he found the magnetisation to be non-uniform. These values are considerably lower than our results, most likely due to his choice of magnetic structure in the non-uniform configuration.

Further experimental characterisation of isolated NPs should be carried out using the X-ray Photo-Emission Electron Microscopy (XPEEM) technique, for example, to probe the magnetic state.[2,3]

ACKNOWLEDGMENTS

This work was supported by Science Foundation Ireland as part of the NISE project, Contract No. 10/IN1.13006 and by IRCSET. The authors thank S. Sen, L. Monzon, M. Venkatesan, and K. Rode for suggestions.

[1]C. Binns *et al.*, "Loss of long-range magnetic order in a nanoparticle assembly due to random anisotropy," J. Phys.: Condens. Matter **20**(5), 055213 (2008).
[2]F. Rodriguez *et al.*, "Size-dependent spin structures in iron nanoparticles," Phys. Rev. Lett. **104**, 127201 (2010).
[3]F. Kronast *et al.*, "Element-specific magnetic hysteresis of individual 18 nm Fe nanocubes," Nano Lett. **11**(4), 1710–1715 (2011).
[4]L. J. Heyderman *et al.*, "Arrays of nanoscale magnetic dots: Fabrication by x-ray interference lithography and characterization," Appl. Phys. Lett. **85**(21), 4989–4991 (2004).
[5]S. Morup *et al.*, "Magnetic nanoparticles," Compr. Nanosci. Technol. **1**, 437–491 (2001).
[6]Z. Diao *et al.*, "Vortex states in soft magnets in two and three dimensions," J. Magn. Magn. Mater. **322**(9–12), 1304–1306 (2010).
[7]D. R. Fredkin and T. R. Koehler, "Numerical micromagnetics of small particles," IEEE Trans. Magn. **24**(6), 2362–2367 (1988).
[8]W. F. Brown, Jr., "The fundamental theorem of fine ferromagnetic particle theory," J. Appl. Phys. **39**, 993 (1968).
[9]A.-H. Lu *et al.*, "Magnetic nanoparticles: Synthesis, protection, functionalization, and application," Angew. Chem., Int. Ed. **46**(8), 1222–1244 (2007).
[10]V. Novosad *et al.*, "Effect of interdot magnetostatic interaction on magnetization reversal in circular dot arrays," Phys. Rev. B **65**, 060402 (2002).
[11]N. A. Usov and S. E. Peschany, "Magnetization curling in a fine cylindrical particle," J. Magn. Magn. Mater. **118**(3), L290–L294 (1993).